Perron, J. T., Myrow, P. M., Huppert, K. L., Koss, A. R., Wickert, A. D. (2018): Ancient record of changing flows from wave ripple defects. - *Geology*, *46*, 10, pp. 875—878.

DOI: http://doi.org/10.1130/G45463.1

Ancient record of changing flows from wave ripple defects

J. Taylor Perron[1], Paul M. Myrow[2], Kimberly L. Huppert[1*], Abigail R. Koss[1†], and Andrew D. Wickert[3]

[1] Department of Earth, Atmospheric & Planetary Sciences, Massachusetts Institute of Technology, Cambridge, Massachusetts 02139, USA
[2] Department of Geology, Colorado College, Colorado Springs, Colorado 80903, USA
[3] Department of Earth Sciences and Saint Anthony Falls Laboratory, University of Minnesota, Minneapolis, Minnesota 55455, USA
[*] Current address: Helmholtz Centre Potsdam, German Research Centre for Geosciences (GFZ), Potsdam 14473, Germany
[†] Current address: Department of Civil and Environmental Engineering, Massachusetts Institute of Technology, Cambridge, Massachusetts 02139, USA

CITATION: Perron, J.T., Myrow, P.M., Huppert, K.L., Koss, A.R., and Wickert, A.D., 2018, Ancient record of changing flows from wave ripple defects: Geology, v. 46, p. 875–878, https://doi.org/10.1130/G45463.1

ABSTRACT

Symmetric sand ripples formed by water waves are common features on modern coasts and in sedimentary rocks. The size and spacing of wave ripples generally scale with water depth and wave conditions, and are widely used to reconstruct coastal environments of the geologic past. Interpretations based on average ripple dimensions and assumed constant wave conditions are informative, but many rippled beds contain striking patterns involving defects—deviations from straight, evenly spaced ripple crests—that suggest more dynamic flow regimes. We report a set of laboratory experiments that reveal how these patterns form in rippled beds adjusting to a change in wave conditions. As the ripples in our experiments evolved toward a new spacing, they developed defects that are widely observed in modern environments and in the rock record. The dominant defect type depends on the sign and magnitude of the adjustment in ripple spacing and the number of wave periods since the change in wave conditions. A regime diagram summarizing these associations quantitatively links ripple defects to transient flow conditions. Our experiments reveal the origin of previously unexplained ripple patterns and add a new dimension to paleoenvironmental interpretations.

INTRODUCTION

Symmetric wave ripples are the most common bedforms in wave-dominated environments, and abound in the rock record. Wave ripples grow when oscillating flows driven by water waves create an instability in a sand bed (Bagnold and Taylor, 1946; Blondeaux, 1990). Ancient ripples can serve as paleoenvironmental indicators (Allen, 1981; Clifton and Dingler, 1984) and have been used to infer extraordinary weather during Earth's most extreme climate excursions (Allen and Hoffman, 2005) and as evidence of ancient flowing water on Mars (Squyres et al., 2004).

Hydraulic interpretations typically focus on the equilibrium characteristics of straight-crested wave ripples, but many ripple fields contain morecomplicated patterns that have not yet been deciphered. The equilibrium spacing of wave ripple crests, λ, is proportional to the orbital diameter (double the amplitude), d_o, of the oscillating flow ($\lambda \approx 0.65 d_o$) up to a critical ratio of d^o to grain size (Bagnold and Taylor, 1946; Miller and Komar, 1980; Pedocchi and García, 2009). The orbital diameter is in turn a function of wave size and water depth (Evans, 1942; Dean and Dalrymple, 1991). However, wave conditions often change faster than ripple spacing adjusts, and therefore wave ripples in nature are often out of equilibrium (Traykovski, 2007). Ancient and modern wave ripples contain a variety of defects (Figs. 1A–1D) that may be signatures of disequilibrium, but the origins of these defects are poorly understood (Kocurek et al., 2010).

Laboratory experiments have revealed how defects accommodate wave ripple adjustment to changing flow conditions along one-dimensional profiles in the direction of wave propagation (Shulyak, 1963; Lofquist, 1978; Davis et al., 2004; Sekiguchi and Sunamura, 2004; Smith and Sleath, 2005; Doucette and O'Donoghue, 2006), similar to the role of defects in the adjustment of river dunes (Venditti et al., 2005a). Modeling studies of two-dimensional (plan view) bedform patterns have similarly shown that defects can nucleate and accommodate changes in ripple spacing (Werner and Kocurek, 1999; Huntley et al., 2008). However, it is not clear how these mechanisms relate to the diverse two-dimensional wave ripple defects commonly observed in the field (Figs. 1A–1D) (Evans, 1943; Boyd, Forbes and Heffler, 1988; Traykovski et al., 1999). In this study, we use laboratory experiments to uniquely associate individual defect types with specific changes in wave conditions. Deciphering wave ripple defects makes it possible to identify dynamic flow transitions in ancient coastal environments, modern systems, and, potentially, in planetary landscapes.

WAVE TANK EXPERIMENTS

We conducted a set of laboratory wave tank experiments to document the response of rippled beds to changes in oscillatory flow. In each experiment, we grew a bed of ripples in equilibrium with a wave-driven flow, subjected the ripples

to a sudden step change in the flow orbital diameter, and recorded their response in plan view with time-lapse photography.

We performed our experiments in a closed-end acrylic tank 60 cm wide, 50 cm deep, and 7 m long. The tank was filled with 5 cm of fine sand (median grain diameter, D_{50} = 0.18 mm) and 40 cm of 20 °C water. At one end of the tank, an electric motor oscillated a hinged paddle, generating waves across the free water surface (see Movie DR1 in the GSA Data Repository[1]). We varied the speed and range of motion of the paddle to produce waves with different amplitudes and periods. At the opposite end of the tank, a sloping "beach" covered with rubberized horsehair minimized wave reflections. A spotlight illuminated the bed at an oblique angle. A sensor on the motor triggered a digital camera to take a downward-looking image of the bed every 10–15 wave cycles. We measured wave period and wave amplitude during the experiments and used linear wave theory (Dean and Dalrymple, 1991) to calculate near-bed velocities and orbital diameter, which ranged from 9.9 to 17.5 cm/s and 5.3–18.8 cm, respectively. Wave periods ranged from 1.5 to 3.5 s, typical of shallow nearshore conditions (Miller and Komar, 1980).

We began each experiment by generating a level sand bed with grooves spaced 1 cm apart perpendicular to the flow to accelerate ripple growth. We subjected this bed to constant wave conditions until ripples with an even, time-invariant spacing formed. We then changed wave conditions to alter the orbital diameter and observed the defects that developed as the ripples adjusted to a new equilibrium spacing. We ran each experiment for 16–33 h (23,000–62,000 wave periods), until ripple spacing and defect abundance stopped changing rapidly.

We measured average ripple spacing throughout each experiment by finding the highest peak in the two-dimensional Fourier power spectrum of each time-lapse image of the bed (Perron et al., 2008), rendered in grayscale to highlight the ripple crests. We also measured spectral entropy (Inouye et al., 1991) to quantify the variability of ripple crest orientation and spacing in each image, and to gauge the prevalence of defects throughout each experiment. Finally, we qualitatively described the dominant defect types as a function of time since the change in wave conditions. Experimental data (Perron et al., 2016; Table DR1) are available at the SEAD Repository (sead-data.net).

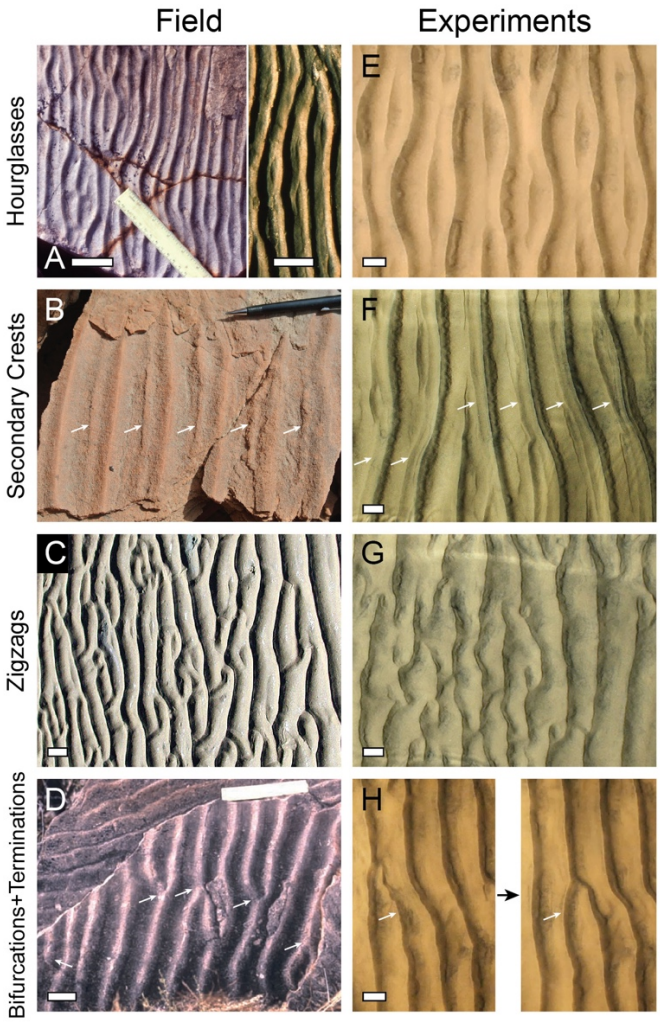

Figure 1. Wave ripple defects in the field (A–D) and in a laboratory wave tank (E–H). Scale bars are 5 cm. A: Hourglass shapes in the Cambrian of Newfoundland (left, photo by P.M. Myrow) and the Proterozoic Tochatwi Formation, Northwest Territories, Canada (right, photo by Paul Hoffman). B: Secondary crests in the Proterozoic of Inner Mongolia (photo by P.M. Myrow). C: Sinuous, broken crests on a beach in Sea Rim State Park, Texas, USA (photo by Zoltán Sylvester). D: Bifurcating and terminating crests in the Proterozoic Apache Group, Arizona (photo by P.M. Myrow). E: Hourglass shapes in ripples transitioning to a narrower spacing due to a reduction in flow orbital diameter. F: Secondary crests formed in response to a larger reduction in orbital diameter than in E. G: Sinuous, broken crests in ripples transitioning to a wider spacing due to an increase in orbital diameter. H: Propagation of a bifurcated crest toward the right by edge dislocation. Right panel shows a later time in the same experiment. Illumination is from the left in all wave tank images.

RESULTS AND DISCUSSION

Adjustment of Ripple Spacing

Ripples that grew from the nearly planar initial bed had few defects and mostly straight, evenly spaced crests (Figs. 2A, 2E, and 2I). After we abruptly changed the wave conditions, the ripples rapidly developed abundant defects as crest spacing and orientation became more variable (Figs. 2B, 2F, and 2J). This proliferation of defects coincided with the start of a monotonic change in ripple spacing and, in most experiments, an increase in spectral entropy (Fig. DR1). As the ripples reached a new equilibrium spacing, the defects

[1] GSA Data Repository item 2018321, additional figures, table, and movies, is available online at www.geosociety.org/pubs/ft2018.htm, or on request from editing@geosociety.org or Documents Secretary, GSA, P.O. Box 9140, Boulder, CO 80301, USA

began to disappear, creating straighter, more evenly spaced crests (Figs. 2C, 2G, and 2K), and spectral entropy generally declined, though the bed still contained some defects long after the average spacing had equilibrated.

Characteristic Defects for Widening and Narrowing Ripple Spacing

The abundance of defects in each experiment followed the general trend described above, but the types of defects varied with the wave forcing and evolved over the course of each experiment. Some defect types were uniquely associated with the sign (widening or narrowing) and magnitude of the change in ripple spacing. Widening ripple spacing caused initially straight crests to become sinuous, and many of these sinuous crests broke into discontinuous segments (Figs. 1G, 2B, and 2C; Movie DR2). The sinuous crests, which we refer to as zigzags, resemble the zigzag instabilities observed in other nonlinear systems that form elongated features, such as Rayleigh-Bénard convection rolls (Cross and Hohenberg, 1993). The average ripple spacing then increased as broken crest segments either lost elevation and disappeared or merged with other segments to create new, continuous crests.

As ripple spacing widened, the evolving beds also frequently developed circular or elliptical depressions with sharp rims, which we call cups (Fig. 2C). Cups, which may be distinct from the closed loops sometimes found on ripple crests (Huntley et al., 2008), typically formed adjacent to a ripple crest, migrated across the crest, and then dissipated, or, less commonly, persisted as stationary features. Although cups were much more common in experiments with widening ripple spacing, they also occasionally appeared in experiments with narrowing ripple spacing.

The dominant defect types in experiments with narrowing ripple spacing depended on the degree of narrowing. For minor to moderate narrowing (35%), new secondary crests formed parallel to, and on either side of, each existing crest (Figs. 1F and 2J) and then migrated toward the troughs as they grew in height, sometimes replacing preexisting crests. In each experiment, the secondary crests on either the right or the left sides of all troughs survived, and those on the opposite sides disappeared (Nienhuis et al., 2014) (Fig. 2K; Movie DR4). The percent narrowing of ripple spacing above which parallel secondary crests formed, instead of hourglasses, in our experiments corresponds approximately to the threshold change in wave conditions required to form double, instead of single, secondary crests identified in previous experiments (Lofquist, 1978; Sekiguchi and Sunamura, 2004). Those experiments, which focused on one-dimensional ripple evolution, were conducted in tanks too narrow to allow hourglasses to form. Double secondary crests can also form on unidirectional flow bedforms, both during adjustment and under steady flow (Allen, 1973; Jerolmack and Mohrig, 2005).

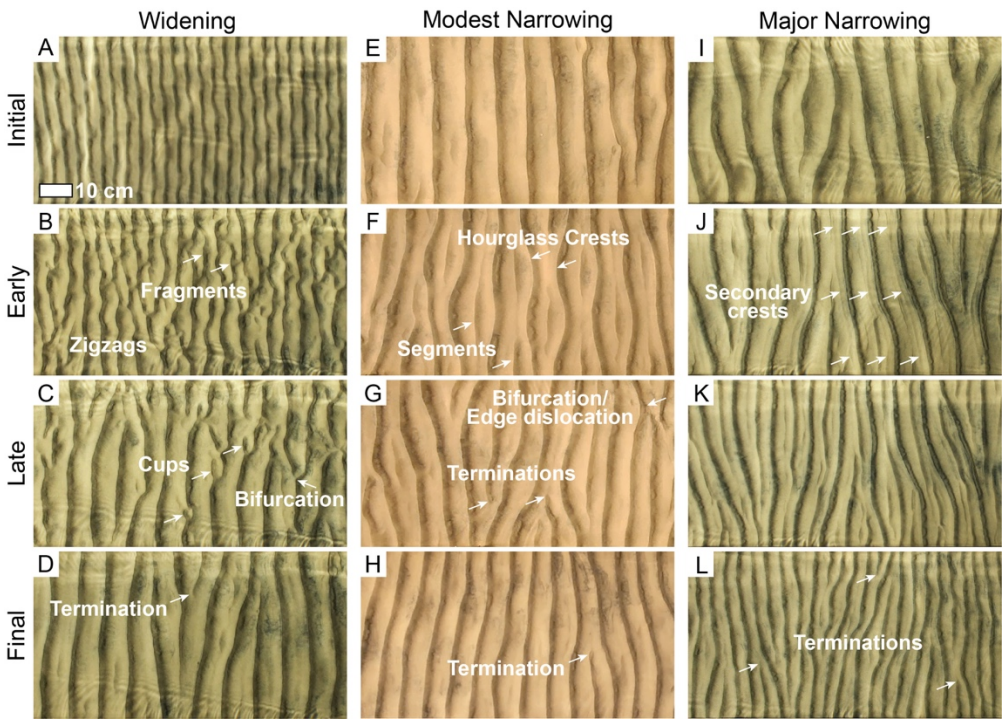

Figure 2. Time-lapse images of three experiments showing widening ripple spacing (A–D), modest narrowing of ripple spacing (E–H), and major narrowing of ripple spacing (I–L). These experiments illustrate the development and eventual elimination of characteristic defects shown in Figure 1, including zigzag crests (B,C; Figures 1C and 1G), hourglass crests (F; Figures 1A and 1E), and secondary crests (J K; Figures 1B and 1F). 10 cm scale bar in A applies to all panels. Illumination is from the left. Time-lapse animations are included in Movies DR2 (A–D), DR3 (E–H), and DR4 (I–L) (see footnote 1).

In some of the experiments involving relatively small changes in ripple spacing (10% narrowing to 20% widening), the defects described above did not form, and ripple spacing adjusted primarily by lateral migration of parallel, unbroken crests. This mechanism of ripple spacing adjustment has been called slide by previous authors (Smith and Sleath, 2005; Doucette and O'Donoghue, 2006) and resembles the stretching or compression observed in some unidirectional flow bedforms (Venditti et al., 2005b). It tended to occur in our experiments when defects in the initial bed were especially sparse.

After the ripple spacing reached a new equilibrium, and the initial defect types mentioned above—zigzags, hourglasses, and secondary crests—disappeared, a different set of dominant defect types persisted, regardless of the sign and magnitude of the change in ripple spacing. These included crest terminations (Figs. 2D, 2H,

and 2L) and bifurcated crests resembling tuning forks (Figs. 1H and 2C). These defects sometimes propagated across the bed via edge dislocations (Fig. 1H; Movie DR5), similar to defects propagating through a crystal lattice—a phenomenon also seen in wind ripples and dunes (Ewing and Kocurek, 2010).

Regime Diagram for Transient Wave Ripple Defects

To quantify the association of different wave ripple defect types with specific disequilibrium conditions, we compiled a regime diagram that generalizes our experimental results (Fig. 3). The dominant defect type on the bed depends mainly on the sign and magnitude of the change in ripple spacing [measured by the quantity $(\lambda f - \lambda i)/\lambda i$, where λi and λf denote the initial and final ripple spacing, respectively] and the number of wave periods following the change in wave conditions. In addition to showing the separation of characteristic defect types by $(\lambda f - \lambda i)/\lambda i$ and the general late-stage transition to bifurcations, terminations, and edge dislocations, the regime diagram also shows that defect types vary in efficiency. Hourglasses require the most wave periods to adjust the ripple spacing, secondary crests require the fewest, and zigzags require an intermediate and more variable number of wave periods (Fig. 3). The abundance of bifurcations and terminations generally declined in the late stages of each experiment, such that straight, evenly spaced crests came to dominate the bed.

In some cases, multiple defect types occurred side-by-side in the same experiment, such as hourglasses and secondary crests (Fig. 1F). This coexistence is also observed in the field (Fig. 1A). Thus, the boundaries in Figure 3 represent transitions in the dominant defect types, not transitions in their exclusive occurrence. An exception may be the boundary between hourglasses and zigzags at $(\lambda f - \lambda i)/\lambda i = 0$; we did not observe any experiments in which both defect types occurred.

Some of the defects we observed (zigzags and secondary crests) resemble the “bulging” and “doubling” patterns that Hansen et al. (2001a, 2001b) produced by oscillating a tray of pre-molded, defect-free ripples at different amplitudes and frequencies. However, a comparison of defects observed in our experiments and theirs as a function of specific flow changes reveals substantial differences (Fig. DR2). We also did not observe the “stability balloon” reported by Hansen et al. (2001a, 2001b) and observed in some one-dimensional experiments (Lofquist, 1978; Sekiguchi and Sunamura, 2004), in which small changes in flow amplitude produced no change in ripple spacing. We attribute these differences to the distinct flows and ripple shapes produced by free-surface waves and oscillating trays (Miller and Komar, 1980; Vongvisessomjai, 1984; Southard, 1991) and the tendency of minor initial defects—which are nearly always present in nature—to facilitate changes in ripple spacing.

Implications for Preservation and Interpretation of Wave Ripple Patterns

Our findings make it possible to reconstruct the transient evolution of ancient and modern coastal environments. All of the defects described here abound in modern sedimentary settings and in the rock record (Figs. 1A–1D), consistent with the interpretation that wave ripples are often adjusting to changing flow conditions. Based on linear wave theory, an increase in flow orbital diameter that generates zigzags (Figs. 1C and 1G) could result from a decrease in water depth or an increase in wave height or length. A decrease in orbital diameter that generates hourglasses (Figs. 1A and 1E) or secondary

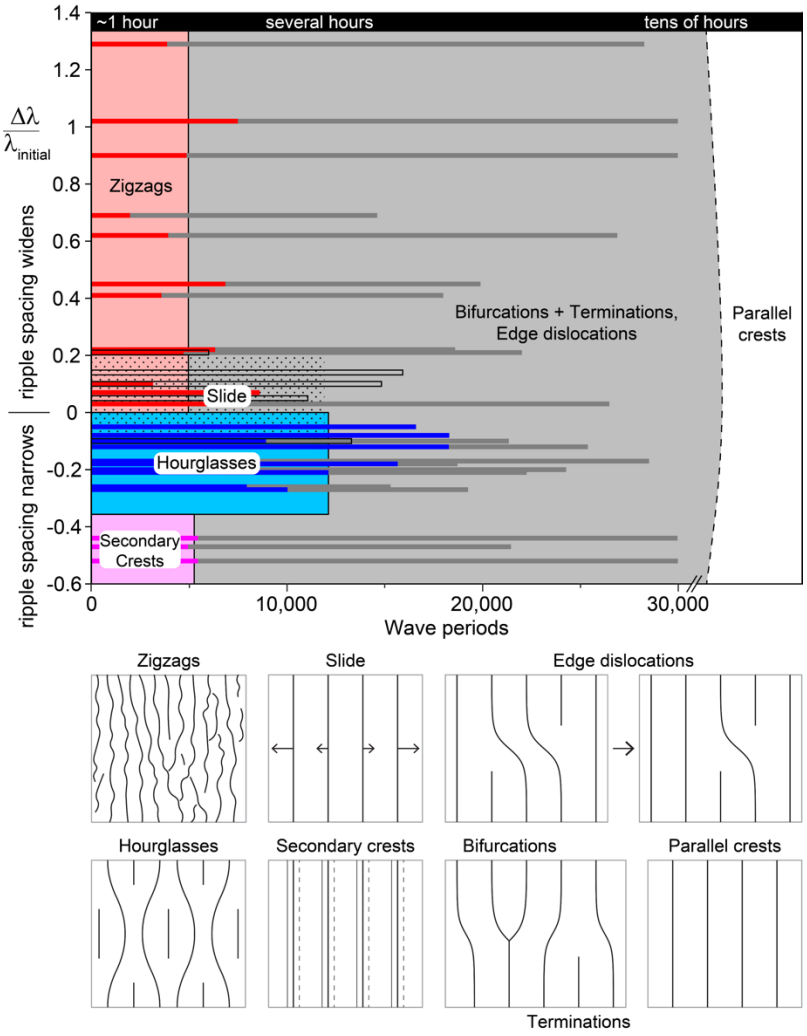

Figure 3. Regime diagram for wave ripple defects. Each horizontal bar represents one wave tank experiment, with the bar color indicating the dominant defect type. Open bars indicate slide. Shaded regions indicate conditions in which the labeled defect types generally dominate. The dashed boundary is speculative. Labels at the top indicate the approximate cumulative time in our experiments. Line drawings below illustrate the various defect types. Dashed secondary crests disappear quickly, leading to the state shown in Figures 1B, 1F, and 2J.

crests (Figs. 1B and 1F) could result from an increase in water depth or a decrease in wave height or length. Because of these associations, certain defects may be more common in particular environments. For example, in lower shoreface or offshore settings, ripples formed by storm waves would likely contain hourglasses or secondary crests created by waning wave sizes at the end of the storm. Nearshore wave ripples formed during a falling tide with constant winds would likely contain zigzags.

Our experiments also provide an explanation for the relative abundance of different defect types in the rock record. Defects that form as the ripple spacing adjusts—zigzags, hourglasses, and secondary crests—are short-lived, persisting for several hours or less in most of our experiments (Fig. 3). The relative longevity of terminating and bifurcating crests suggests that they are more likely to be preserved in rocks, an expectation that is consistent with our field observations (Fig. 1D).

CONCLUSIONS

Hydraulic interpretations of wave-formed sand ripples have largely focused on straight-crested ripples formed under equilibrium conditions, but many rippled beds contain defects that have not yet been deciphered. Our experiments reproduced commonly observed ripple defects, allowing us to construct a regime diagram that links defect types to cumulative wave action and the sign and magnitude of changes in ripple spacing. This link opens a new window onto transient flow conditions in ancient environments and modern sedimentary systems, with potential extensions to bedforms on other planetary bodies.

ACKNOWLEDGMENTS

We thank Michael Szulczewski, Jocelyn Fuentes, Justin Kao, Mathieu Lapôtre, Tristan White, and Tom Ashley for assistance with experiments; John Southard for advice; Ryan Ewing and Nigel Goldenfeld for their suggestions; and Paul Hoffman and Zoltán Sylvester for granting us permission to use their photographs. Reviews by Jeremy Venditti, Mauricio Perillo, and an anonymous reviewer helped us improve the paper. This study was supported by the U.S. National Science Foundation through award EAR-1225865 to Perron and award EAR-1225879 to Myrow.

REFERENCES CITED

Allen, P.A., 1973, Features of cross-stratified units due to random and other changes in bed forms: Sedimentology, v. 20, p. 189–202, https://doi.org/10.1111/j.1365 -3091.1973.tb02044.x.

Allen, P.A., 1981, Some guidelines in reconstructing ancient sea conditions from wave ripplemarks: Marine Geology, v. 43, p. M59–M67, https://doi.org /10.1016/0025-3227(81)90176-6.

Allen, P.A., and Hoffman, P.F., 2005, Extreme winds and waves in the aftermath of a Neoproterozoic glaciation: Nature, v. 433, p. 123–127, https://doi.org /10.1038/nature03176.

Bagnold, R.A., and Taylor, G., 1946, Motion of waves in shallow water: Interaction between waves and sand bottoms: Proceedings of the Royal Society of London: Series A, Mathematical and Physical Sciences, v. 187, p. 1–18, https:// doi.org/10.1098/rspa.1946.0062.

Blondeaux, P., 1990, Sand ripples under sea waves: Part 1. Ripple formation: Journal of Fluid Mechanics Digital Archive, v. 218, p. 1–17, https://doi.org /10.1017/S0022112090000908.

Boyd, R., Forbes, D.L., and Heffler, D.E., 1988, Time-sequence observations of wave-formed sand ripples on an ocean shoreface: Sedimentology, v. 35, p. 449–464, https://doi.org/10.1111/j.1365-3091.1988.tb00997.x.

Clifton, H.E., and Dingler, J.R., 1984, Wave-formed structures and paleoenvironmental reconstruction: Marine Geology, v. 60, p. 165–198, https://doi.org /10.1016/0025-3227(84)90149-X.

Cross, M.C., and Hohenberg, P.C., 1993, Pattern formation outside of equilibrium: Reviews of Modern Physics, v. 65, p. 851–1112, https://doi.org/10.1103 /RevModPhys.65.851.

Davis, J.P., Walker, D.J., Townsend, M., and Young, I.R., 2004, Wave-formed sediment ripples: Transient analysis of ripple spectral development: Journal of Geophysical Research, v. 109, C07020, https://doi.org/10.1029/2004JC002307.

Dean, R.G., and Dalrymple, R.A., 1991, Water Wave Mechanics for Engineers and Scientists: Singapore, World Scientific, https://doi.org/10.1142/1232.

Doucette, J.S., and O'Donoghue, T., 2006, Response of sand ripples to change in oscillatory flow: Sedimentology, v. 53, p. 581–596, https://doi.org/10.1111/j .1365-3091.2006.00774.x.

Evans, O.F., 1942, The relation between the size of wave-formed ripple marks, depth of water, and the size of the generating waves: Journal of Sedimentary Research, v. 12, p. 31–35,

https://doi.org/10.1306/D4269139-2B26-11D7 -8648000102C1865D.

Evans, O.F., 1943, Effect of change of wave size on the size and shape of ripple marks: Journal of Sedimentary Research, v. 13, https://doi.org/10.1306 /D4269189-2B26-11D7-8648000102C1865D.

Ewing, R.C., and Kocurek, G.A., 2010, Aeolian dune interactions and dune-field pattern formation: White Sands Dune Field, New Mexico: Sedimentology, v. 57, p. 1199–1219, https://doi.org/10.1111/j.1365-3091.2009.01143.x.

Hansen, J.L., van Hecke, M., Ellegaard, C., Andersen, K.H., Bohr, T., Haaning, A., and Sams, T., 2001a, Stability balloon for two-dimensional vortex ripple patterns: Physical Review Letters, v. 87, p. 204301, https://doi.org/10.1103 /PhysRevLett.87.204301.

Hansen, J.L., van Hecke, M., Haaning, A., Ellegaard, C., Haste Andersen, K., Bohr, T., and Sams, T., 2001b, Pattern formation: Instabilities in sand ripples: Nature, v. 410, p. 324, https://doi.org/10.1038/35066631.

Huntley, D.A., Coco, G., Bryan, K.R., and Murray, A.B., 2008, Influence of “defects” on sorted bedform dynamics: Geophysical Research Letters, v. 35, L02601, https://doi.org/10.1029/2007GL030512.

Inouye, T., Shinosaki, K., Sakamoto, H., Toi, S., Ukai, S., Iyama, A., Katsuda, Y., and Hirano, M., 1991, Quantification of EEG irregularity by use of the entropy of the power spectrum: Electroencephalography and Clinical Neurophysiology, v. 79, p. 204–210, https://doi.org/10.1016/0013-4694(91)90138-T.

Jerolmack, D.J., and Mohrig, D., 2005, A unified model for subaqueous bed form dynamics: Water Resources Research, v. 41, W12421, https://doi.org/10.1029 /2005WR004329.

Kocurek, G., Ewing, R.C., and Mohrig, D., 2010, How do bedform patterns arise? New views on the role of bedform interactions within a set of boundary conditions: Earth Surface Processes and Landforms, v. 35, p. 51–63, https://doi .org/10.1002/esp.1913.

Lofquist, K.E.B., 1978, Sand Ripple Growth in an Oscillatory-Flow Water Tunnel: U.S. Army Corps of Engineers, Coastal Engineering Research Center Technical Paper 78–5.

Miller, M.C., and Komar, P.D., 1980, A field investigation of the relationship between oscillation ripple spacing and the near-bottom water orbital motions: Journal of Sedimentary Research, v. 50, p. 183–191, https://doi.org/10.2110/jsr.50.183.

Nienhuis, J.H., Perron, J.T., Kao, J.C.T., and Myrow, P.M., 2014, Wavelength selection and symmetry breaking in orbital wave ripples: Journal of Geophysical Research: Earth Surface, v. 119, p. 2239–2257, https://doi.org/10.1002 /2014JF003158.

Pedocchi, F., and García, M.H., 2009, Ripple morphology under oscillatory flow: 1. Prediction: Journal of Geophysical Research, v. 114, C12, https://doi.org /10.1029/2009JC005354.

Perron, J.T., Kirchner, J.W., and Dietrich, W.E., 2008, Spectral signatures of characteristic spatial scales and nonfractal structure in landscapes: Journal of Geophysical Research, v. 113, F04003, https://doi.org/10.1029/2007JF000866.

Perron, J.T., Myrow, P.M., Huppert, K.L., Koss, A.R., and Wickert, A., 2016, Wave Ripple Time-Lapse Experiments: SEAD Repository, https://doi.org /10.5967/M0QR4V39.

Sekiguchi, T., and Sunamura, T., 2004, A laboratory study of formative conditions for characteristic ripple patterns associated with a change in wave conditions: Earth Surface Processes and Landforms, v. 29, p. 1431–1435, https://doi.org /10.1002/esp.1139.

Shulyak, B.A., 1963, Periodic bottom structures of wave flow: Deep Sea Research and Oceanographic Abstracts, v. 10, p. 488–497, https://doi.org/10.1016/0011 -7471(63)90512-6.

Smith, D., and Sleath, J.F.A., 2005, Transient ripples in oscillatory flows: Continental Shelf Research, v. 25, p. 485–501, https://doi.org/10.1016/j.csr.2004.10.012.

Southard, J.B., 1991, Experimental determination of bed-form stability: Annual Review of Earth and Planetary Sciences, v. 19, p. 423–455, https://doi.org /10.1146/annurev.ea.19.050191.002231.

Squyres, S.W., et al., 2004, In situ evidence for an ancient aqueous environment at Meridiani Planum, Mars: Science, v. 306, p. 1709, https://doi.org/10.1126 /science.1104559.

Traykovski, P., 2007, Observations of wave orbital scale ripples and a nonequilibrium time-dependent model: Journal of Geophysical Research: Oceans, v. 112, C06026, https://doi.org/10.1029/2006JC003811.

Traykovski, P., Hay, A.E., Irish, J.D., and Lynch, J.F., 1999, Geometry, migration, and evolution of wave orbital ripples at LEO-15: Journal of Geophysical Research: Oceans, v. 104, C1, p. 1505–1524, https://doi.org/10.1029 /1998JC900026.

Venditti, J.G., Church, M.A., and Bennett, S.J., 2005a, On the transition between 2D and 3D dunes: Sedimentology, v. 52, p. 1343–1359, https://doi.org/10.1111 /j.1365-3091.2005.00748.x.

Venditti, J.G., Church, M.A., and Bennett, S.J., 2005b, Bed form initiation from a flat sand bed: Journal of Geophysical Research, v. 110, F01009, https://doi .org/10.1029/2004JF000149.

Vongvisessomjai, S., 1984, Oscillatory ripple geometry: Journal of Hydraulic Engineering, v. 110, p. 247–266, https://doi.org/10.1061/(ASCE)0733-9429 (1984)110:3(247).

Werner, B.T., and Kocurek, G., 1999, Bedform spacing from defect dynamics: Geology, v. 27, p. 727, https://doi.org/10.1130/0091-7613(1999)0272.3.CO;2.